Equivalent Circuit Models for Resonant and PWM Switches

VATCHÉ VORPÉRIAN, MEMBER, IEEE, RICHARD TYMERSKI, MEMBER, IEEE AND FRED C. Y. LEE, SENIOR MEMBER, IEEE

Abstract—**The switching action in quasi-resonant and pulsewidth-modulated (PWM) converters is attributed to a nonlinear three-terminal switching device for which simple circuit models are obtained. These equivalent circuit models render the dc and small-signal analyses of a large class of PWM and quasi-resonant converters analogous to transistor circuit analysis whereby the transistor is replaced by its equivalent circuit model.**

I. Introduction

THE NONLINEAR switching action in pulsewidth-modulated (PWM) and quasi-resonant converters [1]–[3] can be isolated by lumping the passive and active switches in a single three-terminal device which excludes all the linear circuit elements of the converter. In quasi-resonant converters (QRC's) this three-terminal device is called a resonant switch, whereas in PWM converters it is called a PWM switch. The resonant switch can be further classified as a zero-voltage (ZV) or a zero-current (ZC) switch. An equivalent circuit model of this three-terminal device or switch is obtained by determining the relationship between its average terminal voltages and currents. A small-signal model is obtained by determining the relationship between the perturbations in these average terminal quantities.

With an equivalent circuit model of the switch, a new and possibly simpler approach to a large class of dc-to-dc converters is presented. This method is very similar to transistor amplifier circuit analysis whereby the transistor (the three-terminal device) is replaced by its equivalent circuit model. Hence a particular converter is analyzed for dc and small-signal conditions simply by replacing the three-terminal device by its equivalent circuit model.

The primary contribution of this paper is the determination of the small-signal performance of QRC's utilizing the concept of an equivalent circuit model of a three-terminal switching device. Since the concept of a switch model is sufficiently general, its natural extension to PWM converters is presented as well. The analysis of PWM converters is well understood today using the general method of state-space analysis as given by Ćuk and Middlebrook [5], and it is not the intent of this paper to redo their analysis. However, a *switch model* [7]–[9] is so much more versatile and easy to use than a *converter model* that its application to both PWM and quasi-resonant converters is presented. Finally, with a model for both types of switches, comparisons can be made easily.

Manuscript received December 18, 1987; revised August 26, 1988. This paper was presented at the 1987 IEEE International Symposium on Circuits and Systems, Philadelphia, PA, May 4–7.

The authors are with the Virginia Power Electronics Center, Bradley Department of Electrical Engineering, Virginia Polytechnic Institute and State University, Blacksburg, VA 24061.

IEEE Log Number 8927282.

II. PWM and Resonant Three-Terminal Switching Devices

Fig. 1 illustrates how the nonlinear elements in several zero-current-switched (ZCS) quasi-resonant converters can be lumped into a three-terminal device. This three-terminal device is represented symbolically in Fig. 3(a). The terminal designations a, p, and c refer to active, passive, and common, respectively. Fig. 2 represents how the same procedure can be applied to zero-voltage-switched (ZVS) topologies. The three-terminal zero-voltage switching device is represented symbolically in Fig. 3(b). Two points must be made clear now. First, the mere physical connection of a transistor and a diode does not constitute a three-terminal zero-current or zero-voltage switching device *per se*. Such a three-terminal device acts as a zero-voltage or a zero-current switching device only depending upon external circuit conditions, i.e., whether the converter is a zero-voltage or zero-current-switched topology. Second, the only distinction between Fig. 3(a) and (b) is the specification zv or zc on the symbol of the three-terminal switching device. These two points are further illustrated in Figs. 4 and 5. Fig. 4 shows different possible configurations of the active and passive switches of the three-terminal switching device. When the active switch is bidirectional the three-terminal device acts either as a full-wave mode zero-current switching device or a half-wave mode zero-voltage switching device [2], [4]. The relative orientations of the active and passive switches in a particular three-terminal device is immaterial, i.e., the a and p terminals can correspond to either the collector and anode or to the emitter and cathode of the active and passive switches, respectively. This point is illustrated in Fig. 5 for the case of the ZCS resonant buck converter.

The same process of identifying the three-terminal switching device in PWM converters is shown in Fig. 6 for several single-stage and well-known converters [7]–

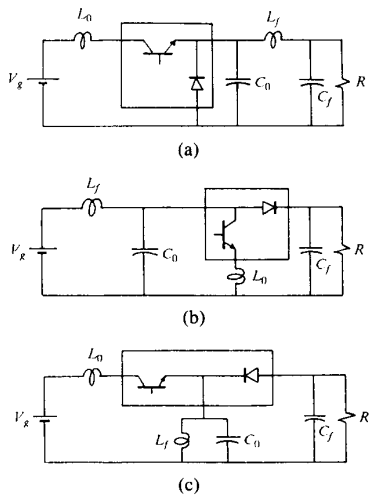

Fig. 1. Three zero-current-switched quasi-resonant converters. (a) Buck. (b) Boost. (c) Buck-boost. Nonlinear switching elements are lumped into three-terminal switching device called zero-current switching device.

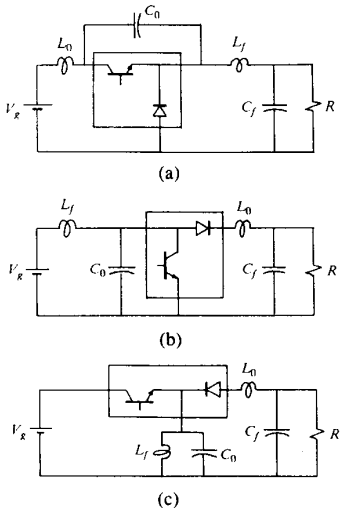

Fig. 2. Three zero-voltage-switched quasi-resonant converters. (a) Buck. (b) Boost. (c) Buck-boost. Nonlinear switching elements are lumped into three-terminal switching device called zero-voltage switching device.

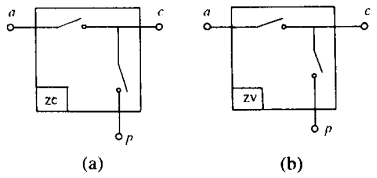

Fig. 3. (a) Symbol for the zero-current switching device. (b) Symbol for zero-voltage switching device.

[9]. This three-terminal switching device is represented symbolically in Fig. 7 where the a, p, c designation is defined as before. The switching action here is represented by a single-pole double-throw switch rather than two single-pole switches as in the case of resonant switches because in PWM converters both switches cannot be on at the same time.

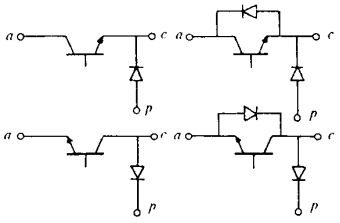

Fig. 4. Four different possible configurations of active and passive switches in three-terminal switching device.

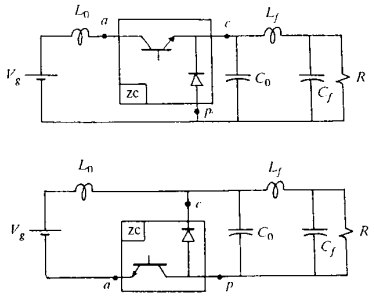

Fig. 5. Two possible configurations of ZCSD in zero-current-switched resonant buck converter. Note that active and passive terminals can correspond to either collector and anode or emitter and cathode of transistor and diode, respectively.

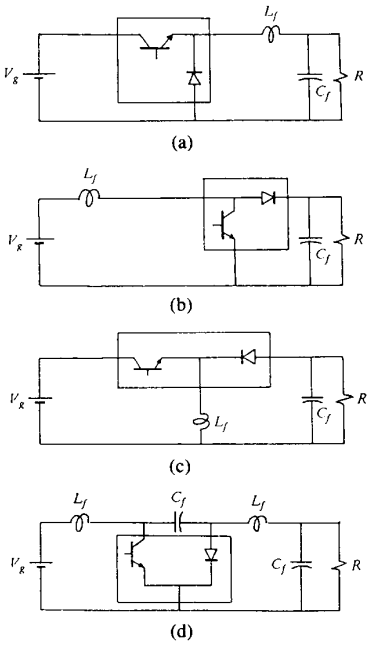

Fig. 6. Four pulsewidth-modulated converters. (a) Buck. (b) Boost. (c) Buck-boost. (d) Ćuk. Nonlinear switching elements are lumped into three-terminal switching device called PWM switch.

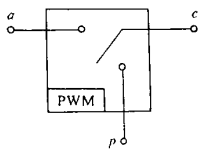

Fig. 7. Symbol for PWM switch.

III. Equivalent Circuit Model of the Zero-Current Switching Device

The three-terminal zero-current switching device (ZCSD) is redrawn in Fig. 8(a) where all the terminal voltages and currents are *average* quantities. The *instantaneous* current $\tilde{i}_a(t)$ is related to the average current i_c, as shown in Fig. 8(b), where t_2 denotes the end of the resonant cycle. Also, the instantaneous voltage $\tilde{v}_{cp}(t)$ is related to the average voltage v_{ap}, as shown in Fig. 8(c), where t_3 denotes the end of the linear discharge cycle. These waveforms can be immediately verified by substituting the ZCSD of Fig. 8(a) in any zero-current-switched converter topology. We have, first, abstracted the switch from the converter and, second, characterized it by its terminal voltages and currents. This last step is a generalization which requires us to see that the same terminal currents and voltages occur no matter which zero-current-switched topology the device is used in, provided that we can write the equations of these terminal waveforms in terms of the average terminal quantities rather than the source and sink quantities. It seems possible then that a circuit model of the three-terminal device can be obtained strictly from the equations of the terminal currents and voltages shown. To do so, consider implementing the ZCSD in the resonant buck converter, as shown in Fig. 9. We can think of this as the "common-passive" configuration of the ZCSD. Clearly, we could have chosen any other configuration we liked. From the results given in [1], [2], or [4] we can deduce that (Appendix I)

$$\frac{v_{cp}}{v_{ap}} = \frac{1}{2\pi}\frac{f_s}{f_0} f(\alpha_c, n) = \mu_c \tag{1}$$

where f_s is the switching frequency and $f_0 = 1/2\pi\sqrt{L_0C_0}$ is the resonant frequency. In this derivation it is assumed that the parasitic elements in the external circuit are negligible. The function $f(\alpha, n)$ is defined here as the *quasi-resonant function* and is given by

$$f(\alpha, n) = \frac{\alpha}{2} + n\pi - (-1)^n \sin^{-1}\alpha + \frac{1}{\alpha} - (-1)^n\sqrt{\frac{1}{\alpha^2} - 1}. \tag{2}$$

In (1) $\alpha = \alpha_c$ where

$$\alpha_c = g_{ac}Z_0 \tag{3a}$$

$$Z_0 = \frac{1}{G_0} = \sqrt{\frac{L_0}{C_0}} \tag{3b}$$

$$g_{ac} = \frac{i_c}{v_{ap}} \tag{3c}$$

$$n = \begin{cases} 2 & \text{full-wave mode} \\ 1 & \text{half-wave mode.} \end{cases} \tag{4}$$

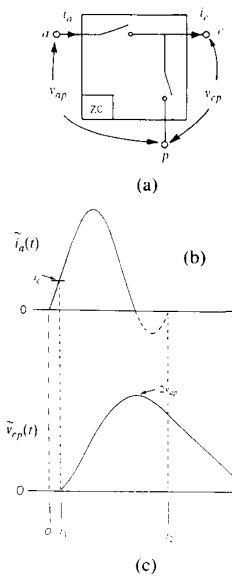

Fig. 8. (a) Terminal voltages and currents of ZCSD. All indicated quantities are average quantities. (b) Instantaneous current $\tilde{i}_a(t)$ in active terminal and its relationship to average current i_c in common terminal. (c) Instantaneous common-to-passive terminal voltage $\tilde{v}_{cp}(t)$ and its relationship to average active-to-passive terminal voltage v_{ap}.

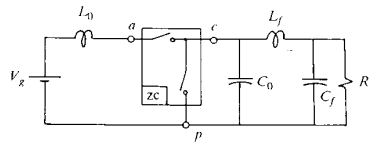

Fig. 9. Implementation of ZCSD in zero-current-switched buck quasi-resonant converter. Model of ZCSD derived in text using this configuration is referred to as "common-passive" model.

Assuming 100-percent efficiency of the three-terminal device, we can write

$$\frac{i_a}{i_c} = \frac{v_{cp}}{v_{ap}} = \mu_c. \tag{5}$$

Equations (1) and (5) describe the average voltage and current gains of the ZCSD. The average circuit model of the ZCSD now follows from (1) and (5) and is shown in Fig. 10.

DC Model of the ZCSD

A steady-state or dc model of the ZCSD follows immediately from Fig. 10, whereby all the quantities are replaced by their dc values, as shown in Fig. 11. These dc quantities are represented by upper case letters or upper case subscripts and are given by

$$\mu_C = \frac{1}{2\pi}\frac{F_s}{F_0} F(\alpha_C, n) = \frac{I_a}{I_c} = \frac{V_{cp}}{V_{ap}} \tag{6}$$

$$\alpha_C = G_{ac}Z_0 \qquad G_{ac} = \frac{I_c}{V_{ap}}. \tag{7}$$

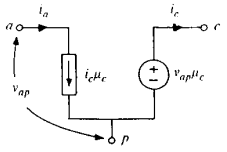

Fig. 10. Average equivalent circuit model of ZCSD in "common-passive" configuration.

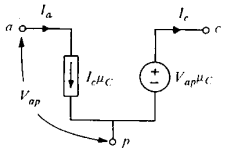

Fig. 11. DC equivalent circuit model of ZCSD.

Small-Signal Model of the ZCSD

Equations (1) and (3) are now perturbed. These perturbations include perturbations in the switching frequency and the average terminal currents and voltages. First, (1) is rewritten and perturbed as

$$v_{cp} = \frac{1}{2\pi}\frac{f_s}{f_0} f(\alpha_c, n) v_{ap} \tag{8}$$

$$\hat{v}_{cp} = \frac{1}{2\pi}\frac{F_s}{F_0} F(\alpha_C, n)\hat{v}_{ap} + \frac{V_{ap}}{2\pi} F(\alpha_C, n)\frac{\hat{f}_s}{F_0} + \frac{V_{ap}}{2\pi}\frac{F_s}{F_0}\frac{\partial f}{\partial \alpha_C} d\alpha_c, \tag{9}$$

but from (3a)–(3c) we have

$$\hat{\alpha}_c \equiv d\alpha_c = \hat{i}_c \frac{Z_0}{V_{ap}} - \hat{v}_{ap}\frac{Z_0 I_c}{V_{ap}^2}. \tag{10}$$

Equations (9) and (10) give

$$\hat{i}_c = -\hat{v}_{cp} g_0 + \hat{v}_{ap} g_f + \hat{f}_c k_0 \tag{11}$$

where

$$\hat{f}_c = \frac{\hat{f}_s}{F_s} \tag{12a}$$

$$g_0 = -\frac{G_0}{\frac{1}{2\pi}\frac{F_s}{F_0}\frac{\partial f}{\partial \alpha_c}} \tag{12b}$$

$$g_f = G_{ac} + \mu_C g_0 \tag{12c}$$

$$k_0 = g_0 V_{cp} \tag{12d}$$

$$\frac{\partial f}{\partial \alpha_c} = \frac{1}{2} - \frac{1}{\alpha_C^2} + (-1)^n \frac{1}{\alpha_C^2}\sqrt{1-\alpha_C^2}. \tag{12e}$$

Clearly, (12b)–(12e) are evaluated at the operating point $(\alpha_C, F_s/F_0)$. Next, we perturb (5) and obtain

$$\hat{i}_a = k_i \hat{f}_c + k_r \hat{i}_c + g_i \hat{v}_{ap} \tag{13}$$

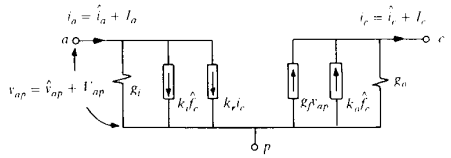

Fig. 12. DC and small-signal equivalent circuit model of ZCSD or ZVSD in "common-passive" configuration. Parameters of model are given in text. In absence of modulation, control sources vanish and model reduces to dc model of ZVSD or ZCSD.

where

$$g_i = -G_0 \frac{\alpha_C^2}{2\pi}\frac{F_s}{F_0}\frac{\partial f}{\partial \alpha_c} \tag{14a}$$

$$k_r = \mu_C - \frac{1}{\alpha_C}\frac{g_i}{G_0} \tag{14b}$$

$$k_i = I_a. \tag{14c}$$

Equations (11) and (13) correspond to the small-signal equivalent circuit model of the ZCSD shown in Fig. 12. This model is also valid for the ZVSD, as will be seen in the next section, but for different values of the parameters.

One should realize that the model given in Fig. 12 is valid for dc conditions as well (with the control dependent sources removed) because the open-loop line-to-output transfer function, obtained by using this model, should have a low frequency asymtote equal to the conversion ratio M of the converter. It can be seen, however, that the easier model to use for dc calculations is the one shown in Fig. 11. An example illustrating the point made in this paragraph is given later on.

Finally, we note that a very useful approximation of (11) and (13) can be made for the case of full-mode operation using the fact that $\alpha < 1$ (and hence $\alpha^2 << 1$). Equations (2) and (12e) for $n = 2$ and under the approximation α less than unity become (Appendix II)

$$f(\alpha, 2) \simeq 2\pi \tag{15}$$

$$\frac{\partial f}{\partial \alpha} \simeq 0. \tag{16}$$

Now (11) and (13) simplify to

$$\hat{v}_{cp} = [\hat{v}_{ap} + V_{ap}\hat{f}_c]\frac{F_s}{F_0} \tag{17}$$

$$\hat{i}_a = I_a \hat{f}_c + \frac{F_s}{F_0}\hat{i}_c. \tag{18}$$

Equations (17) and (18) correspond to the approximate small-signal circuit model shown in Fig. 13 of the ZCSD for full-wave mode of operation. This model is later compared to the model of the PWM switch.

IV. Equivalent Circuit Model of the Zero-Voltage Switching Device

Since the analysis of the ZVSD is similar to the analysis of the ZCSD presented in the previous section, only the

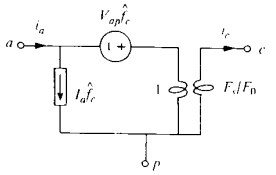

Fig. 13. Approximate dc and small-signal model of ZCSD in full-wave mode of operation for "common-passive" configuration. This model is similar to the model of PWM switch shown in Fig. 20.

final results will be stated here. To derive the model of the ZVSD we implement it in the zero-voltage-switched resonant buck converter, as shown in Fig. 14. The model thus obtained can be thought of as the "common-passive" model of the ZVSD. From the results given in [3], we can deduce that (Appendix I)

$$\frac{i_a}{i_c} = \frac{v_{cp}}{v_{ap}} = 1 - \frac{1}{2\pi}\frac{f_s}{f_0} f(\alpha_v, n) = \mu_v \qquad (19)$$

where

$$\alpha_v = r_{ac} G_0 \qquad r_{ac} = \frac{v_{ap}}{i_c} \qquad (20)$$

and $f(\alpha_v, n)$ is the quasi-resonant function defined in (2). The dc model is shown in Fig. 15. The output circuit parameters of the small-signal model given in Fig. 12 are given by

$$g_0 = -\frac{G_0}{\frac{\alpha_V^2}{2\pi}\frac{F_s}{F_0}\frac{\partial f}{\partial \alpha_v}} \qquad (21a)$$

$$g_f = g_0 \mu_V + G_{ac} \qquad (21b)$$

$$k_0 = -g_0(V_{ap} - V_{cp}) = -g_0 V_{ac}. \qquad (21c)$$

For the input circuit, the parameters are

$$g_i = -G_0 \frac{1}{2\pi}\frac{F_s}{F_0}\frac{\partial f}{\partial \alpha_v} \qquad (22a)$$

$$k_r = \mu_V - \alpha_V \frac{g_i}{G_0} \qquad (22b)$$

$$k_i = I_a - I_c = I_p. \qquad (22c)$$

An approximate model of the ZVSD operating in full-wave mode is easily obtained as explained in the case of the ZCSD. This model is shown in Fig. 16.

V. Analysis of Quasi-Resonant Converters Using the Circuit Model of the Switch

DC Analysis

The conversion-ratio characteristics of the quasi-resonant converters considered in this work can now be easily determined using the dc model of the ZCSD or ZVSD. This method is clearly seen to be analogous to transistor circuit analysis, whereby the transistor is first replaced with its dc equivalent model to determine the dc operating

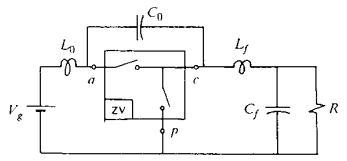

Fig. 14. Implementation of ZVSD in zero-voltage-switched buck quasi-resonant converter. Model of ZVSD derived in text using this configuration is referred to as "common-passive" model.

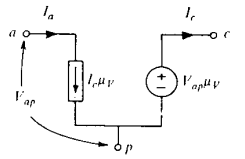

Fig. 15. DC model of ZVSD.

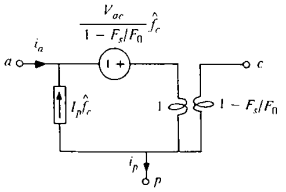

Fig. 16. Approximate dc and small-signal model of ZVSD in full-wave mode for "common-passive" configuration.

point. As an example, consider the zero-current-switched boost resonant converter shown in Fig. 17(a). The ZCSD under dc conditions is replaced by its dc model of Fig. 11, and all reactive elements are either shorted or opened. Thus we obtain the circuit of Fig. 17(b) whence the following can be easily written:

$$V_g = V_{ap}\mu_C + V_0 \qquad V_{ap} = -V_0 \qquad (23)$$

$$M = \frac{V_0}{V_g} = \frac{1}{1 - \mu_C} \quad \text{or} \quad \mu_C = 1 - \frac{1}{M} \qquad (24)$$

but we have from (1)

$$\mu_C = \frac{1}{2\pi}\frac{F_s}{F_0} f(\alpha_C, n) \qquad (25)$$

where

$$\alpha_C = \frac{I_c Z_0}{V_{ap}} = \frac{I_{in} Z_0}{V_0} = \frac{M I_0 Z_0}{V_0} = \frac{Z_0 M}{R} = \frac{M}{Q_p} \qquad (26)$$

and hence we have

$$1 - \frac{1}{M} = \frac{1}{2\pi}\frac{F_s}{F_0} f\left(\frac{M}{Q_p}, n\right). \qquad (27)$$

Thus we have determined the equation for the conversion-ratio characteristics of the zero-current-switched boost resonant converter, for full-wave as well as half-wave modes, without having to analyze the boost converter anew. Following the same procedure the dc characteristics for the other converters given in [1], [2], [3], [6] can be determined. Hence it has been shown that the dc char-

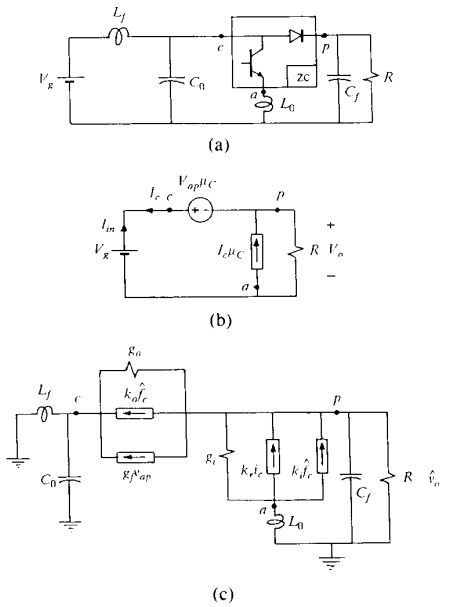

Fig. 17. Boost zero-current-switched quasi-resonant converter. (b) The dc analysis is performed by replacing ZCSD by its dc model of Fig. 11. (c) Small-signal analysis is performed by replacing ZCSD with its equivalent circuit model of Fig. 12.

acteristics of the class of quasi-resonant converters considered here can be determined by using a single circuit model.

It was mentioned earlier that the model of Fig. 12 was equally valid for dc conditions with the control dependent sources removed. We will illustrate this in the next section where we calculate the line-to-output and control-to-output transfer functions. The low-frequency asymptote of the line-to-output transfer function will simply be the conversion ratio M.

Small-Signal Analysis

Once the operating point of a given converter is determined from the dc model, the small-signal analysis can be carried out simply by using the small-signal model of the ZCSD or ZVSD in a manner similar to transistor circuit analysis. As an example, consider the determination of the control-to-output transfer function of the boost converter of Fig. 17(a). The ZCSD is replaced by its equivalent small-signal circuit model of Fig. 12, and the V_g is replaced by a short circuit. The resulting circuit for small-signal analysis is shown in Fig. 17(c). The control-to-output transfer function can be seen to be of fourth order. Upon carrying out the analysis it can be shown that, for frequencies of modulation below half the switching frequency, ($f_m \leq F_s/2$), the desired transfer function can be approximated by a second-order transfer function given by

$$\frac{\hat{v}_0}{\hat{f}_c} \simeq A \frac{1 + \dfrac{s}{s_z}}{1 + \dfrac{s}{\omega_{oc} Q_c} + \dfrac{s^2}{\omega_{oc}^2}} \tag{28}$$

where

$$A = R_p \frac{k_i + k_0(k_r - 1)}{1 + R_p(1 - k_r)(g_0 - g_f)} \tag{29a}$$

$$s_z \simeq \frac{\dfrac{1}{g_0} - \dfrac{Z_0}{\alpha_C}(1 - k_r)}{L_f} \tag{29b}$$

$$\omega_{oc}^2 \simeq \frac{\dfrac{1}{R_p g_0} + (1 - k_r)\left(1 - \dfrac{g_f}{g_0}\right)}{L_f C_f} \tag{29c}$$

$$Q_c \simeq \frac{1}{\omega_{oc}} \frac{(1 - k_r)\left(1 - \dfrac{g_f}{g_0}\right) + \dfrac{1}{R_p g_0}}{\dfrac{L_f}{R_p} + \dfrac{C_f}{g_0}} \tag{29d}$$

where

$$R_p = R \left\| \frac{1}{g_i}. \right. \tag{29e}$$

The approximations involved are simply based on the fact that the relative magnitudes of the components of the resonant filter to the components of the low-pass filter are very small. These approximations though valid, are not necessary unless simple analytic expressions are desired, as given in (28), (29).

Next, we calculate the open-loop line-to-output transfer function simply by placing a perturbation $\hat{v}_g$ at the input as shown in Fig. 17(d) whence one can determine

$$\frac{\hat{v}_0}{\hat{v}_g} \simeq \frac{M}{1 + \dfrac{s}{\omega_{oc} Q_c} + \dfrac{s^2}{\omega_{oc}^2}} \tag{30}$$

where

$$M = \frac{1 + g_i R}{1 - k_r}. \tag{31}$$

We must now show that this M is the same as the one obtained earlier in (24) using the dc model of the switch shown in Fig. 11. We have from (14b) and (26),

$$k_r = \mu_C - \frac{1}{\alpha_C} \frac{g_i}{G_0} = \mu_C - \frac{R g_i}{M}. \tag{32}$$

Substitution of (32) in (31) gives

$$M = \frac{1}{1 - \mu_C}, \tag{33}$$

which is consistent with the result of the dc analysis given earlier in (24).

Experimental and predicted results are shown in Fig. 18. The only difference between full-wave and half-wave mode of operation is the damping. The dependence of the output voltage on the load current in half-wave mode con-

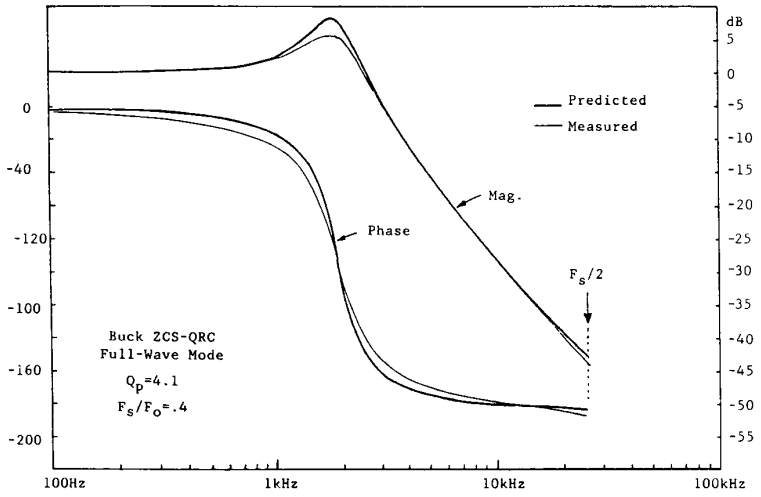

(a)

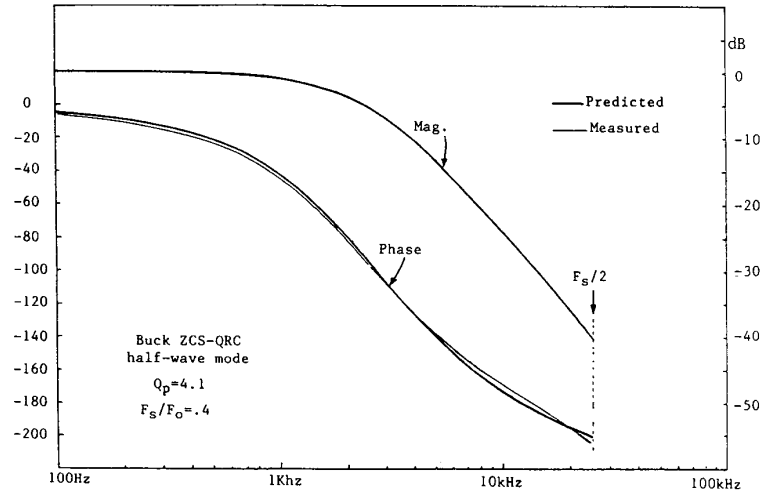

(b)

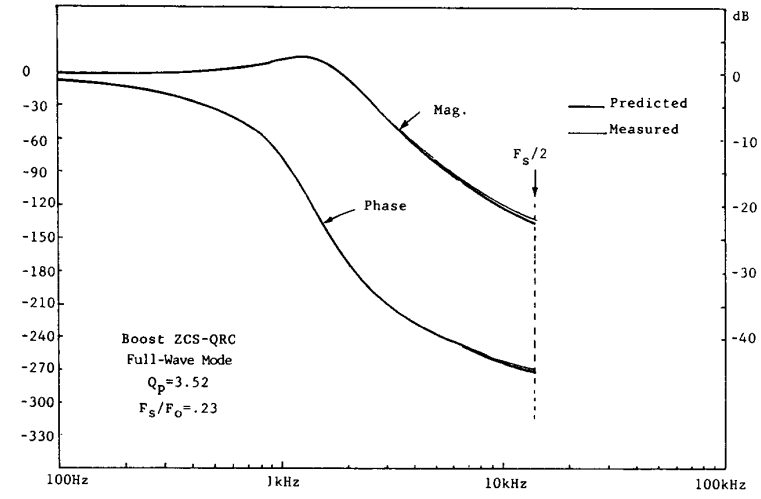

(c)

Fig. 18. Experimental and predicted results for buck and boost ZCS QRC's.

tributes to an incremental internal impedance which causes the extra damping in half-wave mode. Note that in full-wave mode the response is almost identical to the response of the corresponding PWM converters. This will become clear in the next section when we derive the model of the PWM switch.

VI. Equivalent Circuit Model of the PWM Switch

The terminal voltages and currents of a PWM switch operating in continuous conduction mode are in Fig. 19. The relationship between its average terminal voltages and currents are easily seen to be given by

$$v_{ap} = \frac{v_{cp}}{d} \tag{34a}$$

$$i_a = i_c d. \tag{34b}$$

Perturbing (34) we get

$$\hat{v}_{ap} = \frac{\hat{v}_{cp}}{D} - \frac{V_{ap}}{D}\hat{d} \tag{35a}$$

$$\hat{i}_a = I_c\hat{d} + D\hat{i}_c. \tag{35b}$$

These equations correspond to the equivalent circuit model shown in Fig. 20, which is valid for dc and small-signal ac conditions. For dc regime, the control signal sources simply vanish.

A comparison of this model with the approximate model of the ZCSD in full-wave operation reveals that both models are the same with d and f_s/f_0 interchanged. As an application of this model consider the buck–boost converter shown in Fig. 21(a). For dc analysis, the switch is replaced by its dc equivalent model as shown in Fig. 21(b) where all the reactive elements have been shorted or opened. It can be immediately verified from Fig. 21(b) that

$$V_{cp} = V_0 \qquad V_g - V_{ap} = -V_0 \qquad V_{ap} = V_0/D. \tag{36}$$

From these equations the conversion ratio M is found to be

$$M = \frac{V_0}{V_g} = \frac{D}{D'}. \tag{37}$$

Also, we can easily verify that

$$I_c - I_a = I_0 \qquad I_a = I_c D \qquad I_a = \frac{V_0}{RD'}. \tag{38}$$

The small-signal analysis for the determination of the control-to-output transfer function follows by substituting the model of the switch as shown in Fig. 21(c) where V_g has been shorted. Note that the value of the control sources are now determined from the preceding dc analysis. From the circuit in Fig. 21(c) the control-to-output transfer function can be determined and is given by

$$\frac{\hat{v}_0}{\hat{d}} = \frac{V_0}{DD'} \frac{1 - s\dfrac{DL}{D'^2R}}{1 + s/\omega_0 Q + s^2/\omega_0^2} \tag{39}$$

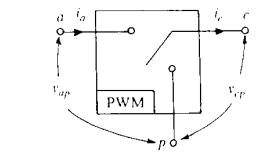

(a)

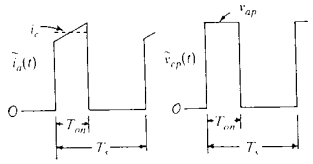

(b)

Fig. 19. (a) PWM switch. (b) Its terminal voltages and currents.

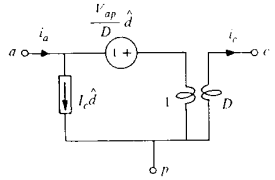

Fig. 20. Equivalent dc and small-signal model of PWM switch in "common-passive" configuration. Under dc conditions small-signal sources vanish.

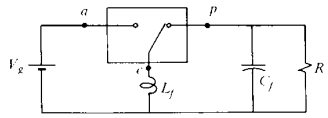

(a)

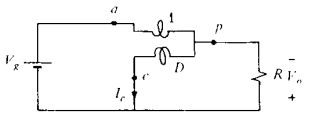

(b)

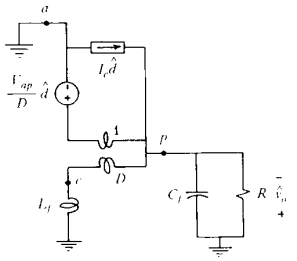

(c)

Fig. 21. (a) Buck-boost PWM converter. (b)-(c) DC and small-signal analyses are performed by replacing PWM switch with its model of Fig. 20.

where

$$\omega_0 = \frac{D'}{\sqrt{LC}} \tag{40a}$$

$$Q = \frac{D'R}{\sqrt{L/C}}. \tag{40b}$$

This result is of course in agreement with the result given in [5] using the method of state-space analysis.

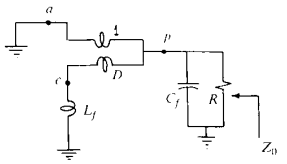

Fig. 22. Determination of output impedance of buck-boost PWM converter.

As another demonstration of the elegance of PWM switch model, consider the determination of the open-loop output impedance of the boost converter. To do so, we simply short V_g to ground as shown in Fig. 22 and obtain

$$Z_0 = \frac{R}{1 + s/\omega_0 Q + s^2/\omega_0^2} \tag{41}$$

where ω_0 and Q are given in (40).

The PWM switch model is discussed in more detail in [8], [9].

VII. Conclusion

The nonlinear switching mechanism in pulsewidth-modulated and quasi-resonant converters has been identified with a three-terminal switching device which consists only of an active and a passive switch. An equivalent circuit model of this switching device describing the perturbations in the average terminal voltages and currents is obtained in both cases. Through the use of this circuit model the analysis of PWM and quasi-resonant converters becomes analogous to transistor circuit analysis whereby the transistor is replaced with its equivalent circuit model.

The conversion-ratio characteristics of various resonant converters and their relationship to a single function, called the quasi-resonant function, is easily obtained using the circuit model for the three-terminal switching device. Also, the small-signal response of quasi-resonant converters to perturbations in the switching frequency and input voltage is determined by replacing the three-terminal switching device by its small-signal equivalent circuit model.

Appendix I

Equations (1) and (19) are no more than the conversion ratio characteristics of the buck ZVS and ZCS quasi-resonant converters as derived by Liu in [1] and [3]. Liu has shown that, for the buck ZCS QRC shown in Fig. 9 the conversion ratio $M = V_0/V_g$ is obtained from the following implicit equation:

$$M = \frac{1}{2\pi}\frac{f_s}{f_0} f\left(\frac{M}{Q_p}, n\right). \tag{42}$$

One can immediately see from Fig. 9 that (ideally) the average voltage v_{cp} is the same as v_0 and the average voltage v_{ap} is the same as V_g. Hence we can refer to the voltage gain of the ZCSD shown in Fig. 9 as

$$\frac{v_{cp}}{v_{ap}} = \frac{1}{2\pi}\frac{f_s}{f_0} f\left(\frac{v_{cp}}{v_{ap}}\frac{1}{Q_p}, n\right) = \mu_c. \tag{43}$$

Since we would like to characterize the ZCSD strictly in terms of its terminal voltages and currents, we write Q_p as follows:

$$Q_p = \frac{R}{Z_0} = \frac{v_0}{i_0}\frac{1}{Z_0} = \frac{v_{cp}}{v_{ap}}\frac{1}{Z_0} \tag{44}$$

whereby we have used the fact that $i_c = i_0$. Substituting (44) in (43) we obtain (1)

$$\frac{v_{cp}}{v_{ap}} = \frac{1}{2\pi}\frac{f_s}{f_0} f(\alpha_c, n) \tag{45}$$

where

$$\alpha_c = \frac{i_c}{v_{ap}} Z_0 = g_{ac} Z_0 \qquad g_{ac} = \frac{i_c}{v_{ap}},$$

Similarly, for the buck ZVS QRC, Liu [3] has shown that M is obtained from

$$M = 1 - \frac{1}{2\pi}\frac{f_s}{f_0} f\left(\frac{Q_p}{M}, n\right), \tag{46}$$

which can be manipulated in the same way as shown above to yield (19). For the derivation of (42) and (46) the reader is referred to [1] and [3].

Appendix II

We would like to show that $F(\alpha, n) \simeq 2\pi$ and $\partial f/\partial\alpha \simeq 0$ for $n = 2$. Consider the expansions

$$\sqrt{1 - \alpha^2} \simeq 1 - \frac{\alpha^2}{2}, \qquad \alpha \le 1 \tag{47}$$

$$\sin^{-1}\alpha \simeq \alpha, \qquad \alpha \le 1. \tag{48}$$

Substituting these in the quasi-resonant function and its derivative given by (2) and (12e), respectively, we get for $n = 2$,

$$f(\alpha, 2) \simeq \frac{\alpha}{2} + 2\pi - \alpha + \frac{1}{\alpha} - \frac{1}{\alpha} + \frac{\alpha}{2} = 2\pi \tag{49}$$

$$\frac{\partial f}{\partial\alpha} \simeq \frac{1}{2} - \frac{1}{\alpha^2} + \frac{1}{\alpha^2}\left(1 - \frac{\alpha^2}{2}\right) = 0. \tag{50}$$

References

[1] K. Liu and F. C. Lee, "Resonant switches: A unified approach to imProving performances of switching converters," in *Proc. INTELEC '84*, IEEE Publ. 84CH2073-5, pp. 344-359.

[2] K. Liu, R. Oruganti, and F. C. Lee, "Resonant switches: Topologies and characteristics," in *IEEE Power Electronics Specialists Conf. 1985 Rec.*, IEEE Publ. 85CH2117-0, pp. 106-116.

[3] K. Liu and F. C. Lee, "Zero-voltage switching technique in dc/dc converters," in *IEEE Power Electronics Specialists Conf. 1986 Rec.*, IEEE Publ. 86CH2310-1, pp. 58-70.

[4] M. M. Jovanović *et al.*, "State-plane analysis of quasi-resonant converters," in *INTELEC Conf. Rec.*, 1985.

[5] R. D. Middlebrook and S. Ćuk, "A general unified approach to modeling switching-converter power stages," in *IEEE Power Electronics Specialists Conf. 1976 Rec.*, IEEE Publ. 76CH1084-AES, pp. 18-34.

[6] V. Vorpérian *et al.*, "Generalized resonant switches Parts I and II," in *Conf. Proc. Virginia Power Electronics Center (VPEC)*, 1986, pp. 116-131.

[7] V. Vorpérian, "Average model of the single-pole double-throw switch in PWM converters," VPEC internal correspondence, Feb. 11, 1986.

[8] ——, "Simplify your PWM converter analysis using the model of the PWM switch. Part I: Continuous conduction mode," VPEC Newsletter, *Current*, Fall 1988.
[9] ——, "Simplify your PWM converter analysis using the model of the PWM switch. Part II: Discontinuous conduction mode," VPEC Newsletter, *Current*, Winter 1989.

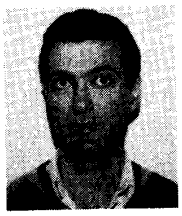

Vatché Vorpérian (S'77-M'77-S'80-S'80-M'83) was born on December 4, 1952. He received the B.S. and M.S. degrees in electrical engineering from Northeastern University, Boston, MA, in 1976 and 1977, respectively, and the Ph.D. degree from the California Institute of Technology, Pasadena.

He worked for Digital Equipment Corporation in Maynard, MA, for two years. In 1979 he joined the Power Electronics Group at California Institute of Technology. Currently, he is an Assistant Professor with the Electrical Engineering Department at Virginia Polytechnic Institute and State University, Blacksburg.

Richard Tymerski (S'87-M'88) received the B.Sc. degree in mathematics and the B.E. and M.Eng.Sc. degrees in electrical engineering from the University of New South Wales, Sydney, Australia, in 1977, 1980, and 1983, respectively, the M.S. degree from the California Institute of Technology, Pasadena, in 1984, and the Ph.D. degree from the Virginia Polytechnic Institute and State University, Blacksburg, in 1988, both in electrical engineering.

During 1980–1983, he worked for Medtel Pty. Ltd. and Newsound Electronics Pty. Ltd. in Sydney, Australia, as an Electronics Design engineer. He is currently on the faculty of the Electrical Engineering Department at Portland State University, OR, where he is an Assistant Professor.

Fred C. Y. Lee (S'72-M'74-M'77-SM'87), for a photograph and biography please see page 204 of this issue.